Supporting Information

Supplementary Texts

Text S1: Details of the flow-through experiments

Reactors were 10 cm in length, 5 cm in width, and 6 cm in height. Each reactor contained 8 pairs of electrodes, and 1mm thick meshed plastic sheets were used to separate the cathodes and anodes. Preliminary experiments guided the use of 0.1 mol/L Na_2SO_4 at pH 2 as the electrolyte (Fig. S6). Upon introducing new electrochemical conditions, the system was given time to stabilize, processing 0.6 L of electrolyte before sampling for analysis.

Text S2: Details of the *in operando* visualization

To set up the *in operando* visualization reactor, a 2×2 cm^2 coverslip was affixed to the base of a modified circuit board which had a central cavity. The coverslip was then used to hold the electrolyte. Further, a 1×1 cm^2 Ir-Ta coated Ti plate was positioned on one side of the coverslip to serve as the anode. To prepare the carbon cathode, active carbon felts were ground into powder firstly. Secondly, the powder was added to the mixture of Nafion, ethanol, and water. Thirdly, drops of the suspension were applied onto the coverslip until there was enough active carbon powder on the coverslip. Finally, the reactor was placed into a 60℃ oven until the suspension on the coverslip was thoroughly dried, and the powder was attached to the coverslip. The electrolyte was prepared by integrating the pH-sensitive fluorescence probe into the

Na_2SO_4 solution (0.1 mol/L, pH = 4). When performing fluorescence imaging with the laser scanning confocal microscope (LSCM), A 63x lens was utilized with a scope field dimension of 134.69 μm × 134.69 μm, and excitation was provided by the AF488 laser channel.

Supplementary Figures

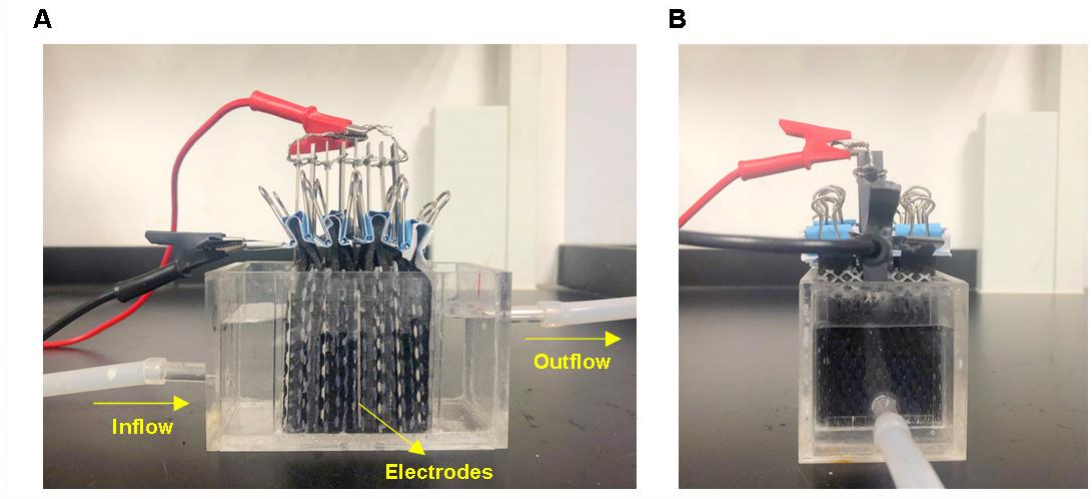

Fig. S1 Digital photos of the flow-through reactor with coupled anodes and cathodes for H_2O_2 electrosynthesis. (A) The front view. (B) The left view.

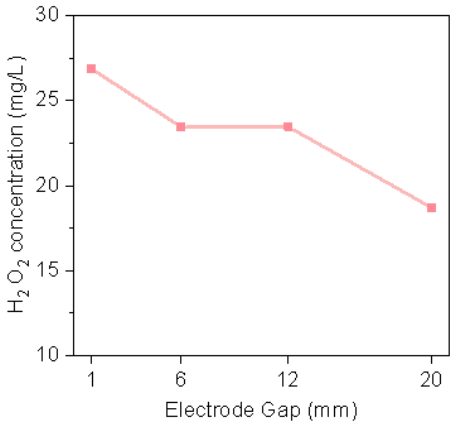

Fig. S2 Effect of electrode gap on H_2O_2 concentration. Three-electrode system, constant 1.5 V vs SHE, sampling at 30 min, the 0.1 mol/L Na_2SO_4 solution at pH 2 was used as the electrolyte.

Note: the anode potential was kept the same to ensure a similar anodic O_2 production. Electrode gap below 1 mm was not tested as a too small electrode spacing will increase the possibility of a short circuit.

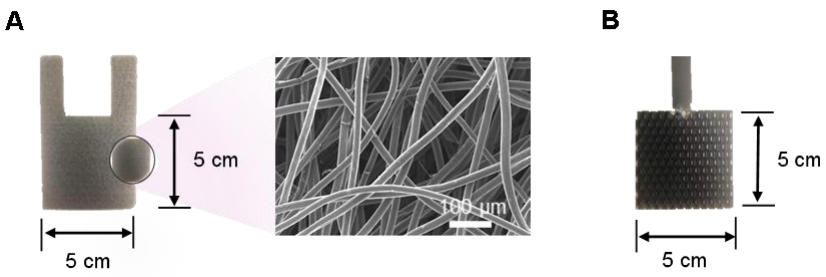

Fig. S3 Electrodes used in H_2O_2 electrosynthesis in the flow-through reactors. (A) Physical diagram and SEM image of the activated carbon felt cathode. (B) Physical diagram of the mesh Ir-Ta coated Ti anode.

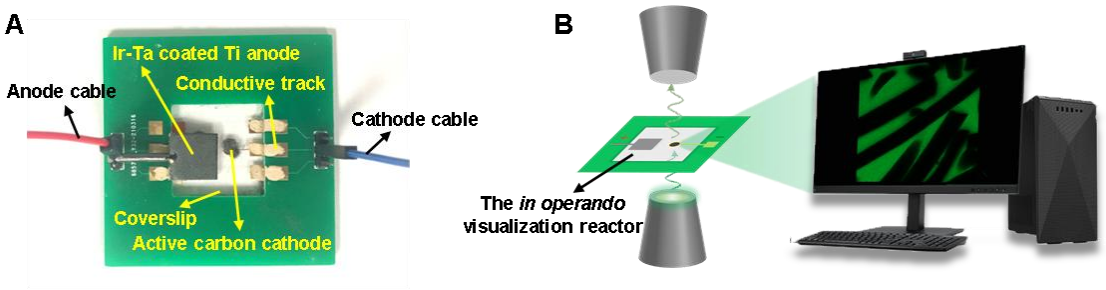

Fig. S4 The *in operando* visualization system. (A) Digital photos of the *in operando* visualization reactor. (B) Schematic of imaging fluorescence intensity at the cathode-solution interface using an LSCM.

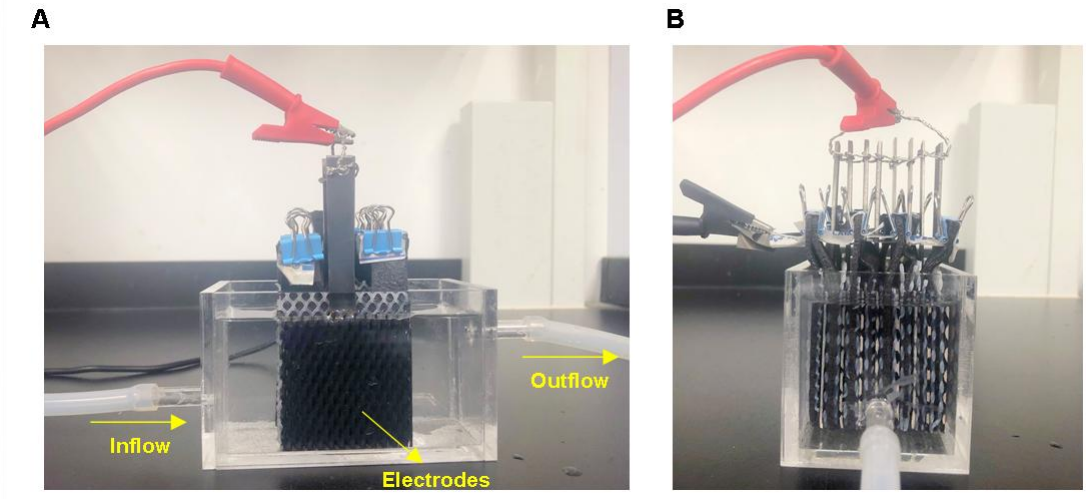

Fig. S5 Digital photos of the reactor with non-coupled anodes and cathodes for H_2O_2 electrosynthesis. (A) The front view. (B) The left view.

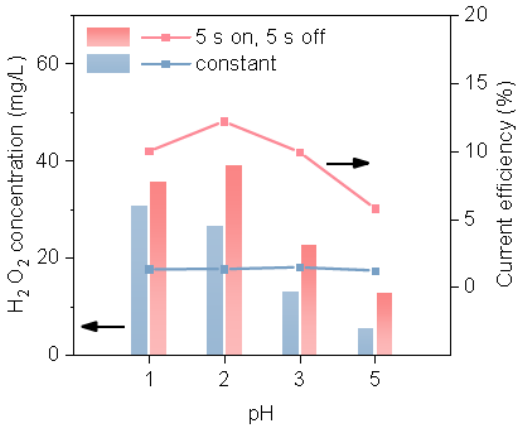

Fig. S6 Effects of pH on H_2O_2 concentration and current efficiency. The 3.0 V constant voltage was applied. The flow rate was 10 mL/min. The 0.1 mol/L Na_2SO_4 solution at different pH levels was used as the electrolyte.

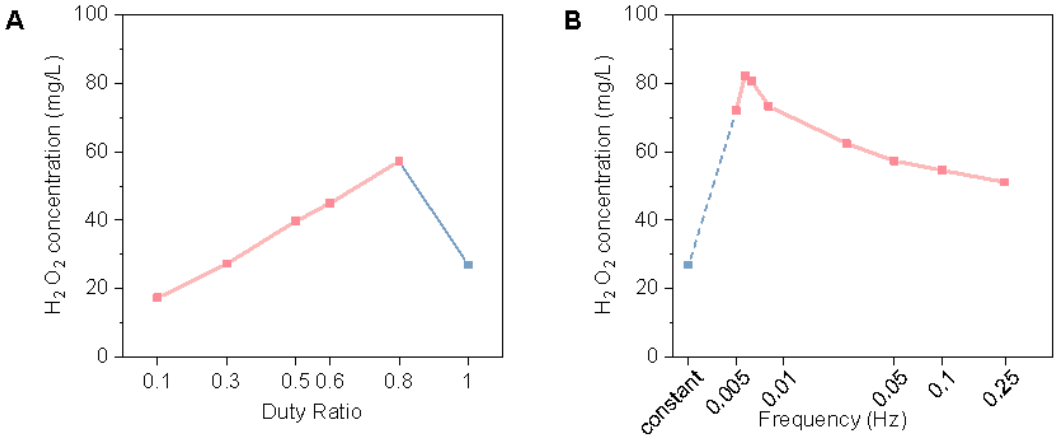

Fig. S7 (A) Effect of duty ratio on H_2O_2 concentration (t_{on} was 5 s). (B) Effects of frequency on H_2O_2 concentration (duty ratio was 0.8). The 3.0 V constant voltage was applied. The flow rate was 10 mL/min. The 0.1 mol/L Na_2SO_4 solution at pH 2 was used as the electrolyte.

Note: Duty Ratio = $t_{on}/(t_{on}+t_{off})$, Frequency = $1/(t_{on}+t_{off})$. Quite large duty ratio (>0.8) and low frequency (<0.01) were observed as the proper condition. For a simple regulation, t_{on} and t_{off} were used as the parameters in the main experiments rather than Duty Ratio and Frequency.

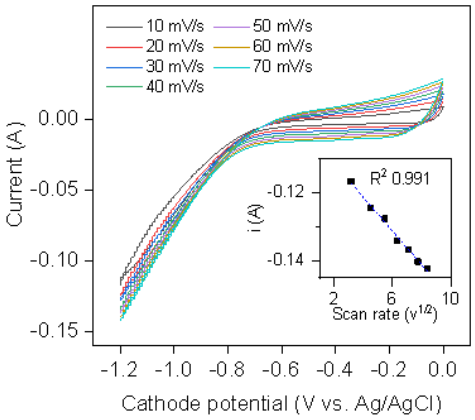

Fig. S8 CV curves of active carbon felts under different scan rates. The three-electrode system was used, where Ir-Ta-Ti, Ag/AgCl, and 0.1 mol/L Na_2SO_4 solution at pH 2 were used as the counter electrode, reference electrode, and electrolyte, respectively.

Note: the peak current i_p (A) increases linearly with the square root of the scan rate $v^{1/2}$ ($V^{1/2}{\cdot}s^{-1/2}$). Therefore, the electrochemical process was indicated to be the the diffusion-controlled according to the Randles-Sevcik equation ($i_p = 0.4463nFAC\left(\frac{nF\nu D}{RT}\right)^{\frac{1}{2}}$) (Ding et al., 2021; Wang et al., 2024).

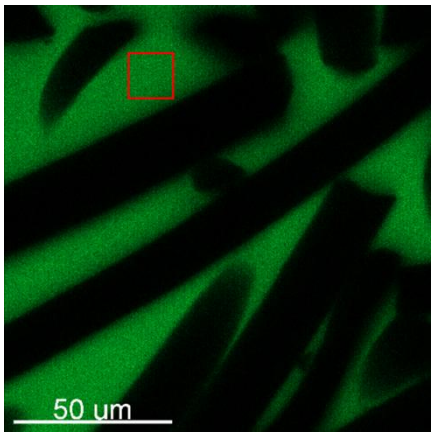

Fig. S9 Selected region for quantitative analysis of fluorescence intensity (red box area in the figure).

Supplementary Table

Table S1 The comparison of H_2O_2 yield, energy consumption, and the reaction system design of this work with the literature.

Cathodes	Reactor design	Aerated or not	H_2O_2 yield (mg/h)	Electric energy consumption (kWh/kg)	Aeration energy consumption (kWh/kg)	**Total energy consumption (Electric + Aeration) (kWh/kg)**	Ref.
Commercial carbon felts	Flow-through	No	15.8 (2mL/min) -168.0 (60mL/min)	13.0 (60mL/min) -146.8 (2mL/min)[a]	0	13.0~146.8	This work
carbon-PTFE GDE	Flow-through	Yes (compressed air)	3894 (pilot scale)	53.9[b]	1077[b]	1130.9	(Salmerón et al., 2019)
Carbon felts	Flow-through	Yes (jet aerator)	76.8[c]	68.75[c]	Not provided	>68.75	(Leyva-Ruiz et al., 2024)
Air self-diffusion electrode	Flow-through	No	7.5[c]	134	0	134	(Zhang et al., 2024)
Modified GDE	Batch	Yes (O_2 saturated)	170.0[c]	118.0	Not provided	>118.0	(Moreira et al., 2019)
Modified GDE	Batch	Yes (0.2 bar O_2)	125.8[c]	84.5	Not provided	>84.5	(Lima et al., 2020)
Modified GDE	Batch	Yes (0.2 bar O_2)	55.5[c]	86.6	Not provided	>86.6	(Cordeiro Junior et al., 2022)
Modified GDE	Batch	Yes (0.05 L/min O_2)	46.0[c]	47.85	Not provided	>47.85	(O. Silva et al., 2023)
Graphite cathode	Batch	No	1.9[c]	213.0-368.8	0	213.0-368.8	(Zhang et al., 2020b)

[a] Parameters used for calculation: the optimal conditions of 3 V, 100 s on and 1 s off. At the fastest flow rate of 60 mL/min, the average current (calculated as $\int Idt\,/t$) was 0.73 A, and the system reached the electric energy consumption of 13.0 kWh/kg. At the slowest flow rate of 2 mL/min, the average current (calculated as $\int Idt\,/t$) was 0.77 A, and the system reached the electric energy consumption of 146 kWh/kg. Electric energy consumption at flow rates among 2-60 ml/min was among 13.0-146.8 kWh/kg, decreasing as the flow rates increased.

[b] Using the calculated results in Zhang et al., 2020a.

[c] Calculated based on the data in the corresponding reference.

References of supporting information

Cordeiro Junior P J M, Martins A S, Pereira G B S, Rocha F V, Rodrigo M a R, Lanza M R D V (2022). High-performance gas-diffusion electrodes for H_2O_2 electrosynthesis. Electrochimica Acta, 430: 141067

Ding Y, Zhou W, Xie L, Chen S, Gao J, Sun F, Zhao G, Qin Y (2021). Pulsed electrocatalysis enables an efficient 2-electron oxygen reduction reaction for H_2O_2 production. Journal of Materials Chemistry A, 9(29): 15948-15954

Leyva-Ruiz D, Treviño-Reséndez J, Godínez L A, Robles I, Acosta-Santoyo G, García-Espinoza J D (2024). Electrochemical degradation of carbamazepine in water by a flow-through and pilot-scale reactor with carbon felt electrodes: Parametric study under realistic operational conditions. Journal of Environmental Chemical Engineering, 12(4): 113232

Lima V B, Goulart L A, Rocha R S, Steter J R, Lanza M R V (2020). Degradation of antibiotic ciprofloxacin by different AOP systems using electrochemically generated hydrogen peroxide. Chemosphere, 247: 125807

Moreira J, Bocalon Lima V, Athie Goulart L, Lanza M R V (2019). Electrosynthesis of hydrogen peroxide using modified gas diffusion electrodes (MGDE) for environmental applications: Quinones and azo compounds employed as redox modifiers. Applied Catalysis B: Environmental, 248: 95-107

O. Silva T, A. Goulart L, Sánchez-Montes I, O. S. Santos G, B. Santos R, Colombo R, R. V. Lanza M (2023). Using a novel gas diffusion electrode based on PL6 carbon modified with benzophenone for efficient H_2O_2 electrogeneration and degradation of ciprofloxacin. Chemical Engineering Journal, 455: 140697

Salmerón I, Plakas K V, Sirés I, Oller I, Maldonado M I, Karabelas A J, Malato S (2019). Optimization of electrocatalytic H_2O_2 production at pilot plant scale for solar-assisted water treatment. Applied Catalysis B: Environmental, 242: 327-336

Wang Z, Liu S, Cui S, Jing B, Qiu S, Deng F (2024). Electrochemical disinfection boosting by a pulsed-assisted MXene-based cathode. Electrochimica Acta, 489: 144232

Zhang Q, Zhou M, Ren G, Li Y, Li Y, Du X (2020a). Highly efficient electrosynthesis of hydrogen peroxide on a superhydrophobic three-phase interface by natural air diffusion. Nature Communications, 11(1)

Zhang S, Yue Z, Pang X, Pan M, Tang J, Cheng X, Li J, Liu Y, Shen W (2020b). In-situ synthesis of hydrogen peroxide using water electrolysis and Pd/MWCNTs catalyst. Desalination and Water Treatment, 179: 387-395

Zhang X, Wang H, Guo Y, Bian Z (2024). Tetracycline degradation through selective activation of molecular oxygen by a fluidic sequential photoelectro-Fenton system. Separation and Purification Technology, 350: 127959